Available online at www.sciencedirect.com

ScienceDirect

Geochimica et Cosmochimica Acta 176 (2016) 227–238

Geochimica et Cosmochimica Acta

www.elsevier.com/locate/gca

Triple oxygen isotopic composition of the high-^{3}He/^{4}He mantle

N.A. Starkey [a,*], C.R.M. Jackson [b], R.C. Greenwood [a], S. Parman [c], I.A. Franchi [a], M. Jackson [d], J.G. Fitton [e], F.M. Stuart [f], M. Kurz [g], L.M. Larsen [h]

[a] Planetary and Space Sciences, The Open University, Walton Hall, Milton Keynes MK7 6AA, UK
[b] Geophysical Laboratory, Carnegie Institution of Washington, 5251 Broad Branch Rd. NW, Washington, DC 20015-1305, USA
[c] Brown University, Providence, RI 02912, USA
[d] Department of Earth Science, UC Santa Barbara, 1006 Webb Hall, Santa Barbara, CA, USA
[e] School of GeoSciences, Grant Institute, The King's Buildings, James Hutton Road, Edinburgh EH9 3FE, UK
[f] SUERC, Rankine Avenue, East Kilbride G75 0QF, UK
[g] Woods Hole Oceanographic Institution, 266 Woods Hole Road, Woods Hole, MA 02543-1050, USA
[h] Geological Survey of Denmark and Greenland, Øster Voldgade 10, DK-1350 Copenhagen K, Denmark

Received 12 August 2015; accepted in revised form 26 December 2015; available online 2 January 2016

Abstract

Measurements of Xe isotope ratios in ocean island basalts (OIB) suggest that Earth's mantle accreted heterogeneously, and that compositional remnants of accretion are sampled by modern, high-^{3}He/^{4}He OIB associated with the Icelandic and Samoan plumes. If so, the high-^{3}He/^{4}He source may also have a distinct oxygen isotopic composition from the rest of the mantle. Here, we test if the major elements of the high-^{3}He/^{4}He source preserve any evidence of heterogeneous accretion using measurements of three oxygen isotopes on olivine from a variety of high-^{3}He/^{4}He OIB locations. To high precision, the $\Delta^{17}O$ value of high-^{3}He/^{4}He olivines from Hawaii, Pitcairn, Baffin Island and Samoa, are indistinguishable from bulk mantle olivine ($\Delta^{17}O^{\text{Bulk Mantle}} - \Delta^{17}O^{\text{High 3He/4He olivine}} = -0.002 \pm 0.004$ (2 × SEM)‰). Thus, there is no resolvable oxygen isotope evidence for heterogeneous accretion in the high-^{3}He/^{4}He source. Modelling of mixing processes indicates that if an early-forming, oxygen-isotope distinct mantle did exist, either the anomaly was extremely small, or the anomaly was homogenised away by later mantle convection.

The $\delta^{18}O$ values of olivine with the highest ^{3}He/^{4}He ratios from a variety of OIB locations have a relatively uniform composition (~5‰). This composition is intermediate to values associated with the depleted MORB mantle and the average mantle. Similarly, $\delta^{18}O$ values of olivine from high-^{3}He/^{4}He OIB correlate with radiogenic isotope ratios of He, Sr, and Nd. Combined, this suggests that magmatic oxygen is sourced from the same mantle as other, more incompatible elements and that the intermediate $\delta^{18}O$ value is a feature of the high-^{3}He/^{4}He mantle source. The processes responsible for the $\delta^{18}O$ signature of high-^{3}He/^{4}He mantle are not certain, but $\delta^{18}O$–$^{87}Sr/^{86}Sr$ correlations indicate that it may be connected to a predominance of a HIMU-like (high U/Pb) component or other moderate $\delta^{18}O$ components recycled into the high-^{3}He/^{4}He source.

1. INTRODUCTION

Noble gases provide evidence for the preservation of a reservoir in the Earth's mantle that has been less melted and degassed than the rest of the mantle (as sampled by mid-ocean ridge basalts, (MORB)). Ocean island basalts from locations such as Iceland, Hawaii and Samoa provide

* Corresponding author.
E-mail address: natalie.starkey@open.ac.uk (N.A. Starkey).

http://dx.doi.org/10.1016/j.gca.2015.12.027

evidence for a mantle component with a higher time-integrated $^{3}He/(U+Th)$ ratio compared to the MORB mantle source (Kurz et al., 1982). This leads to the assumption that the inferred lower mantle source of high-$^{3}He/^{4}He$ OIB is less processed compared to the upper mantle, as typical mantle processing (i.e., melting, degassing, and recycling) acts to decrease $^{3}He/(U+Th)$ (Kurz et al., 1982). This assumption is also supported by experimental work focused on understanding the behaviour of He compared to U + Th during partial melting of the upper mantle (Jackson et al., 2013).

Isotopic systems with short-lived radioactive parent nuclides support the argument that the high-$^{3}He/^{4}He$ mantle source is in fact a compositional heterogeneity preserved from the Earth's accretion. Specifically, a high-$^{3}He/^{4}He$ Icelandic basalt (DICE10; Mukhopadhyay, 2012) and a high-$^{3}He/^{4}He$ basalt from the Lau Basin (Peto et al., 2013) have lower, less radiogenic $^{129}Xe/^{130}Xe$ compared to the MORB mantle source, as previously discussed by Trieloff et al. (2000). The short half-life of ^{129}I (^{129}I decays to ^{129}Xe, $T_{1/2} = 15.7$ Ma) requires that the mantle sources of the DICE10 and Lau Basin samples were isolated from MORB mantle within 80 Ma of calcium–aluminium-rich inclusion (CAI) condensation. Apparently, this early-forming isotopic heterogeneity has not been completely homogenised, indicating relatively long timescales for complete mantle mixing (Mukhopadhyay, 2012; Peto et al., 2013).

Recent observations of $^{182}W/^{184}W$ heterogeneity associated with ancient plumes and other Archean rocks also support the possibility that the lower mantle contains reservoirs formed during Earth's accretion (Touboul et al., 2012). Crucially, the $^{182}W/^{184}W$ heterogeneity observed for Earth is contrasted by $^{182}W/^{184}W$ homogeneity for the Moon (Touboul et al., 2007), suggesting that early-forming reservoirs were not homogenised during the giant impact phase of accretion. A late-forming Moon (formation after the extinction of ^{182}Hf, >50 Ma after CAIs), and hence a late addition of cosmochemically distinct material to Earth, is supported by the age of the oldest lunar zircon (4.417 Ga; Nemchin et al., 2009), the oldest concordant age of lunar anorthosites (4.47 Ga; Nyquist et al., 2010), and the late model ages for the co-differentiation of major lunar geochemical reservoirs (low-Ti mare, high-Ti mare, KREEP, ~4.4 Ga after CAI; McLeod et al., 2014 and references within). We use the term "cosmochemically distinct" to refer to materials with distinct nebular feeding zones, which should result in correspondingly distinct $\Delta^{17}O$ values. Recent modelling efforts also suggest that giant impacts do not necessarily result in whole-mantle homogenisation (Nakajima and Stevenson, 2015).

If such an early-forming reservoir exists, it follows that this reservoir might also have a distinct O isotope composition compared to the rest of the mantle, given the timescales associated with Earth's accretion, i.e., the Moon-forming impactor impacted Earth >50 Ma after CAI formation (Touboul et al., 2007). Oxygen possesses three stable isotopes: ^{16}O, ^{17}O and ^{18}O and these were fractionated by a non-mass dependent process in the solar nebula, producing distinct reservoirs that do not fall along a mass fractionation line (Clayton, 1993; McKeegan et al., 2011).

Meteoritic materials generally display large non-mass dependent variations in O isotope compositions (quantified as variations in $\Delta^{17}O$), when compared to terrestrial samples (Clayton, 1993; Greenwood et al., 2005; Franchi, 2008). Even at a planetary scale, the distinct O isotopic composition of Martian rocks compared to terrestrial materials (Franchi, 2008) suggests that the inner solar system was not completely homogenised with respect to O isotopes. Given that terrestrial planets represent a stochastic mixture of nebular materials (Chambers, 2001; Kaib and Cowan, 2015), this also implies that material accreted to Earth and other terrestrial bodies, such as the Moon-forming impactor, had a range of O-isotope compositions, i.e., they were cosmochemically distinct. If the short-lived Xe isotopic compositions of high-$^{3}He/^{4}He$ OIB are evidence for an unmixed primordial heterogeneity, then it is likely that this heterogeneity also had a non-zero $\Delta^{17}O$ upon formation. That is, high-$^{3}He/^{4}He$ OIB should have O isotopes that fall off the TFL if subsequent interactions with the rest of the mantle were sufficiently small. Since oxygen is a major element, it mixes linearly between silicate reservoirs and has well constrained homogenisation tendencies compared to elements such as Xe or W, which are also potential tracers of materials isolated early in solar system history.

Previous studies of O isotope variation in high-$^{3}He/^{4}He$ material have focused almost entirely on measuring $\delta^{18}O$ and not $\delta^{17}O$, thus precluding the unambiguous identification of cosmochemical distinctions. A low-$\delta^{18}O$ component is commonly associated with plumes displaying high-$^{3}He/^{4}He$ signatures with the ultimate cause of low-$\delta^{18}O$ signatures having been variably attributed to source properties (Macpherson et al., 2000, 2005) or near-surface contamination (Wang and Eiler, 2008). If high-$^{3}He/^{4}He$ mantle has a $\delta^{18}O$ signature distinct from MORB mantle, this might indicate a fundamentally different history for these two reservoirs, potentially related to the distribution of materials recycled in to the mantle.

Here we test the hypothesis that high-$^{3}He/^{4}He$ mantle formed with a distinctive O isotopic signature and has not been completely homogenised since. Measurements of both $\delta^{18}O$ and $\delta^{17}O$ have been made, allowing for the determination of $\Delta^{17}O$ in olivine from a variety of high-$^{3}He/^{4}He$ locations, including in samples from Baffin Island and West Greenland (BI-WG) that exhibit the highest $^{3}He/^{4}He$ measured to date (Stuart et al., 2003; Starkey et al., 2009).

2. MATERIALS AND METHODS

2.1. Samples

The olivine samples obtained for this study are from lava flows from a range of locations including Baffin Island and West Greenland (proto-Iceland plume), Hawaii, Samoa and Pitcairn. These locations were chosen because they are known for having lava flows characterised by high $^{3}He/^{4}He$, and cover a wide range of locations across the

globe (north and south) which are associated with the two separate large low shear velocity provinces.

The BI-WG olivine samples are from picritic lava flows (except BI/CS/7, which is a dyke sample) that are thought to be stratigraphically equivalent, originating from the proto-Iceland plume that erupted 62–58 Ma. It has been shown previously that the Baffin Island dyke sample, BI/CS/7, has experienced a small amount of crustal contamination (Starkey et al., 2009) evidenced by its more enriched Sr and Nd isotopes compared to the rest of the sample suite. The Baffin Island (BI) samples, BI/CS/7 and BI/PI/27, and West Greenland (WG) samples, 400485 and 400230, have not previously been measured for O isotopes but a large range of geochemical data for these samples is presented in Stuart et al. (2003), Starkey et al. (2009, 2012).

The Hawaiian olivines were extracted from samples HSDP2-SR0036-1.22, HSDP2-SR0741-7.90 and HSDP2-SR964-4.31 collected in the Hawaii Scientific Drilling Project. HSDP2-SR741-7.90 and HSDP2-SR964-4.30 have been measured for O isotopes by Wang et al. (2003), helium isotope data for all samples is presented in Kurz et al. (2004), and Sr and Nd isotope data in Bryce et al. (2005).

The Samoan olivines were extracted from samples OFU.04.03 (ankaramite dyke), OFU.04.14 (cumulate), OFU.04.15 (ankaramite) and OFU.04.17 (gabbro). These samples were collected from a range of locations in the Ofu and Olosega islands, in the eastern province of the Samoan archipelago (Jackson et al., 2007). He, Sr, and Nd data for these samples are presented in Jackson et al. (2007). Sr isotopes and $\delta^{18}O$ have previously been measured for OFU.04.17 by Workman et al. (2008).

The Pitcairn olivines were extracted from samples Pitcairn 8 and Pitcairn 16 collected from the Tedside volcanic formation (Garapic et al., 2015). The helium isotope data for these samples is presented in Garapic et al. (2015).

The Icelandic olivines are from sample SK1 which is a Tertiary picrite from Selardalur in NW Iceland. Olivines from this sample have a $^3He/^4He$ value of 37 Ra (Ellam and Stuart, 2004).

In the case of Hawaii, Samoa and Pitcairn, new aliquots of crystals from the same samples that had previously been measured for helium were analysed for their O isotope ratios whereas for BI-WG the same olivine samples that had been analysed by crushing for He were used for the O isotope analyses. The average $^3He/^4He$ values for the BI-WG samples in this study is 44 Ra, the average for Samoan samples is 26 Ra, for Hawaii it is 15 Ra and for Pitcairn it is 12 Ra (all data available in Table 1).

2.2. Oxygen isotope measurements

Oxygen isotope analyses were carried out at the Open University using an infrared laser-assisted fluorination system (Miller et al., 1999). Each replicate analysis was undertaken using approximately 2 mg of crushed olivine crystals that were hand-picked under a binocular microscope. Oxygen was released from the sample by heating in the presence of BrF_5. After fluorination, the released oxygen gas was purified by passing it through two cryogenic nitrogen traps and over a bed of heated KBr. Oxygen gas was analysed using a MAT 253 dual inlet mass spectrometer. Interference at $m/z = 33$ by the NF_3 fragment ion NF^+ was monitored by performing scans for NF_2^+ on all samples run in this study. In all cases NF_2 was either negligible or absent. Recent levels of precision obtained on the Open University system, as demonstrated by 38 analyses of an internal obsidian standard were as follows: ±0.053‰ for $\delta^{17}O$; ±0.095‰ for $\delta^{18}O$; ±0.018‰ for $\Delta^{17}O$ (2 SD), with full results available in supplementary information.

Oxygen isotopic analyses are reported in standard δ notation, where $\delta^{18}O$ has been calculated as: $\delta^{18}O = [(^{18}O/^{16}O_{sample})/(^{18}O/^{16}O_{ref}) - 1] \times 1000$ (‰) and similarly for $\delta^{17}O$ using the $^{17}O/^{16}O$ ratio. $\Delta^{17}O$, which represents the deviation from the terrestrial fractionation line, has been calculated using a linearised format:

$$\Delta^{17}O = 1000\ln(1 + \delta^{17}O/1000) - \lambda\ 1000\ln(1 + \delta^{18}O/1000)$$

where $\lambda = 0.5247$, which was determined using 47 terrestrial whole-rock and mineral separate samples (Miller et al., 1999). When calculating $\Delta^{17}O$ values, Pack and Herwartz (2014) have advocated abandoning the use of slope values (λ) calibrated using natural silicate minerals and instead propose a significantly steeper slope of 0.5305, the theoretical maximum for equilibrium fractionation, with a y axis offset of 0. This approach is problematic in view of the fact that a wide range of studies demonstrate that the majority of natural silicates on Earth plot on slopes which vary between 0.5240 and 0.5250 (Miller et al., 2015). Here we retain the use of a λ value of 0.5247 as this is based on well constrained analytical data (Miller et al., 1999; Miller, 2002). For the $\Delta^{17}O$ comparisons reported here, the importance of choosing the proper λ is minimised because we compare $\Delta^{17}O$ values of samples with very similar $\delta^{18}O$ values.

In this paper we are concerned with comparing the mean isotopic values, i.e., $\delta^{18}O$ and $\Delta^{17}O$, of mantle reservoirs that may have potentially remained isolated from each other since Earth accretion. In order to indicate the level of uncertainty of these mean values, the errors quoted throughout this paper, unless otherwise indicated, are two times the standard error of the mean (2 × SEM), where standard error of the mean (SEM) = standard deviation (SD)/$\sqrt{n}$ (where n = number of measurements). Values for both the SD and SEM for all samples analysed in this study are given in Table 1.

During the course of this study both internal (obsidian) and international standards (UWG-2 garnet, NBS-28, San Carlos olivine) were run alongside the olivine samples. For reference, the full dataset obtained for UWG-2 garnet, NBS-28 and the internal obsidian standards, run over the course of this study, are included as a table in supplementary information. The average values we obtained for UWG-2 garnet and NBS-28 were $\delta^{18}O = 5.78$‰ and 9.59‰, which are extremely close to the recommended values (also available in table in supplementary information). In theory, San Carlos olivine would be the most appropriate standard for this study, being closest in mineralogical composition to the high-$^3He/^4He$ olivine samples. Literature $\delta^{18}O$ values for San Carlos range from 4.70‰ to 5.28‰, which is not a particularly wide variation when

Table 1
Triple oxygen isotope compositions as measured by laser fluorination for a range samples from Iceland, Baffin Island, West Greenland, Hawaii and Samoa plus average values for these and for the standards San Carlos olivine and PSRI Obsidian. $^3He/^4He$ values measured in previous studies are provided as reference.

Sample	Location	*n*	$^3He/^4He$	$\delta^{17}O‰$	SD	SEM	$\delta^{18}O‰$	SD	SEM	$\Delta^{17}O‰^{\dagger}$	SD	SEM	$\Delta^{17}O‰^{\dagger\dagger}$	SD	SEM
All samples															
PIT8	Pitcairn	2	8	2.728	0.020	0.014	5.248	0.045	0.031	−0.001	0.003	0.002	−0.022	0.004	0.002
PIT16	Pitcairn	2	16	2.677	0.020	0.014	5.125	0.028	0.019	0.012	0.005	0.004	−0.009	0.005	0.004
SK1	Iceland	12	37.7	2.158	0.076	0.022	4.139	0.148	0.043	0.005	0.008	0.002	−0.012	0.008	0.002
BI/P1/27	Baffin Island	9	43.1	2.669	0.050	0.017	5.119	0.088	0.029	0.007	0.011	0.004	−0.014	0.011	0.004
BI/CS/7	Baffin Island	3	43.9	2.661	0.032	0.018	5.067	0.060	0.035	0.026	0.013	0.008	0.006	0.013	0.008
400230	West Greenland	12	47.6	2.602	0.069	0.020	4.989	0.130	0.038	0.008	0.007	0.002	−0.012	0.007	0.002
400485	West Greenland	11	40.3	2.602	0.058	0.017	4.992	0.104	0.031	0.006	0.011	0.003	−0.014	0.011	0.003
HSDP2-SR0036-1.22	Hawaii	6	8.4	2.659	0.103	0.042	5.076	0.186	0.076	0.019	0.012	0.005	−0.001	0.012	0.005
HSDP2-SR964-4.31	Hawaii	6	12.5	2.586	0.045	0.018	4.959	0.092	0.038	0.007	0.008	0.003	−0.013	0.008	0.003
HSDP2.SR0741-7.90	Hawaii	6	23.9	2.561	0.054	0.022	4.906	0.106	0.043	0.010	0.012	0.005	−0.010	0.012	0.005
OFU.04.03	Samoa	7	24	2.582	0.069	0.026	4.950	0.119	0.045	0.008	0.015	0.006	−0.012	0.015	0.006
OFU.04.14	Samoa	10	25	2.635	0.058	0.018	5.043	0.107	0.034	0.012	0.007	0.002	−0.008	0.007	0.002
OFU.04.15	Samoa	11	29.6	2.650	0.063	0.019	5.073	0.108	0.032	0.012	0.014	0.004	−0.009	0.014	0.004
OFU.04.17	Samoa	8	26.4	2.647	0.047	0.017	5.068	0.095	0.034	0.012	0.010	0.003	−0.009	0.010	0.003
Average values		105		2.601	0.135	0.013	4.982	0.258	0.025	0.010	0.006	0.001	−0.010	0.006	0.001
San Carlos Olivine I ($\delta^{18}O = 4.88‰$)		19		2.487	0.067	0.015	4.768	0.133	0.030	0.008	0.009	0.002	−0.012	0.010	0.002
San Carlos Olivine II ($\delta^{18}O = 5.23‰$)		9		2.674	0.054	0.018	5.130	0.096	0.032	0.007	0.010	0.003	−0.014	0.010	0.003
PSRI Obsidian		39		3.808	0.026	0.004	7.267	0.047	0.007	0.029	0.009	0.001	0.001	0.009	0.001
High $^3He/^4He$ olivines = >20 Ra and >4.75 $\delta^{18}O$ (see text for full definition)															
BI/P1/27	Baffin Island	9	43.1	2.669	0.050	0.017	5.119	0.088	0.029	0.007	0.011	0.004	−0.014	0.011	0.004
400230	West Greenland	12	47.6	2.602	0.069	0.020	4.989	0.130	0.038	0.008	0.007	0.002	−0.012	0.007	0.002
400485	West Greenland	11	40.3	2.602	0.058	0.017	4.992	0.104	0.031	0.006	0.011	0.003	−0.014	0.011	0.003
HSDP2.SR741.90	Hawaii	6	23.9	2.561	0.054	0.022	4.906	0.106	0.043	0.010	0.012	0.005	−0.010	0.012	0.005
OFU.04.03	Samoa	7	24	2.582	0.069	0.026	4.950	0.119	0.045	0.008	0.015	0.006	−0.012	0.015	0.006
OFU-04-14	Samoa	10	25	2.635	0.058	0.018	5.043	0.107	0.034	0.012	0.007	0.002	−0.008	0.007	0.002
OFU.04.15	Samoa	11	29.6	2.650	0.063	0.019	5.073	0.108	0.032	0.012	0.014	0.004	−0.009	0.014	0.004
OFU.04.17	Samoa	8	26.4	2.647	0.047	0.017	5.068	0.095	0.034	0.012	0.010	0.003	−0.009	0.010	0.003
Average values		74		2.619	0.037	0.004	5.017	0.071	0.008	0.010	0.002	0.000	−0.011	0.002	0.000
"Bulk Mantle" $\delta^{18}O‰$ (Mattey et al., 1994)		76					5.18	0.14	0.02						
"Bulk Mantle" $\Delta^{17}O‰$ (Average San Carlos I and II)		28											−0.012	0.01	0.002

Notes:
SD = sample standard deviation.
SEM = standard error of the mean.
SEM was calculated as: $SEM = SD/\sqrt{n}$.
n = number of measurements.
† $\Delta^{17}O = \delta^{17}O - 0.52\ \delta^{18}O$.
†† Linearized value: see text for details.

compared to other standards (UWG-2 garnet, NBS-28 quartz, NBS-30 biotite) (Kusakabe and Matsuhisa, 2008). Such variation would normally be ascribed to inter-laboratory analytical differences. However, San Carlos olivine is not a homogenous standard and distinct isotopic varieties exist (Thirlwall et al., 2006), which may be related to the mineralogy or metasomatic history of the particular nodule sampled from the San Carlos locality. For this study we obtained two samples of San Carlos olivine, a low $\delta^{18}O$ variety, referred to as San Carlos I by Thirlwall et al. (2006), with a $\delta^{18}O$ value of 4.88‰ (Mattey and Macpherson, 1993) and a high $\delta^{18}O$ variety, San Carlos II, assigned a value of $\delta^{18}O = 5.22$‰ by Thirlwall et al. (2006). The results of our analysis of San Carlos I and II are given in Table 1. Nineteen analyses of San Carlos I gave a $\delta^{18}O$ value of 4.768 (±0.060)‰, which is just over 0.1‰ lower than the value of $\delta^{18}O = 4.88$‰ obtained by Mattey and Macpherson (1993). Nine replicate analyses of San Carlos II gave a $\delta^{18}O$ value of 5.130 (±0.064)‰, which is just under 0.1‰ lower than the assigned value quoted by Thirlwall et al. (2006). However, the five analyses of San Carlos II given in Table 3 of Thirlwall et al. (2006) have a mean value of 5.19 (±0.06)‰, which indicates that the apparent offset between our analysis of San Carlos II and that of Thirlwall et al. (2006) is probably not statistically significant. It would appear that further work is required to adequately assess the use of San Carlos as a reliable interlaboratory isotopic standard. However, despite San Carlos olivine not being a well-characterised international standard, the close compositional match between it and the olivines analysed in this study make it a useful standard with respect to $\Delta^{17}O$.

3. RESULTS

3.1. O isotopes in high-$^3He/^4He$ samples

Despite their differing $\delta^{18}O$ values, the two fractions of San Carlos olivine measured in this study (San Carlos I and II) both have identical $\Delta^{17}O$ values within error (Table 1). Furthermore, the recent study of Pack and Herwartz (2014) indicates that San Carlos olivine lies along a common mass fractionation line with the other minerals within San Carlos xenoliths and MORB glass (Pack and Herwartz, 2014). This suggests that San Carlos olivine can be used as a proxy for the $\Delta^{17}O$ of the bulk mantle. We use the term "bulk mantle" to denote the mantle other than high-$^3He/^4He$ mantle. For the $\delta^{18}O$ measurements we also plot the average mantle value reported by Mattey et al. (1994) of 5.18 ± 0.28‰ ($n = 76$, 2 S.D) (Table 1) to provide a frame of reference.

Fig. 1 displays the new $\Delta^{17}O$ and $\delta^{18}O$ measurements for olivines from a range of locations with variable $^3He/^4He$ ratios up to 47.6 Ra. High-$^3He/^4He$ olivines show no deviation from the bulk mantle mean $\Delta^{17}O$ value (within 2σ SEM), as defined by replicate analyses of San Carlos olivine. To high precision, there is no resolvable difference between the $\Delta^{17}O$ average of San Carlos olivine and the $\Delta^{17}O$ average of high $^3He/^4He$ olivine (Fig. 1, $\Delta^{17}O^{\text{San Carlos olivine}} - \Delta^{17}O^{\text{high }^3He/^4He\text{ olivine}} = -0.002 \pm 0.004$ (2 SEM)‰). A Baffin Island sample (BI/CS/7) is the only one to fall off the main trend, to a positive value of $\Delta^{17}O$ and this measurement also has a larger error than the other samples.

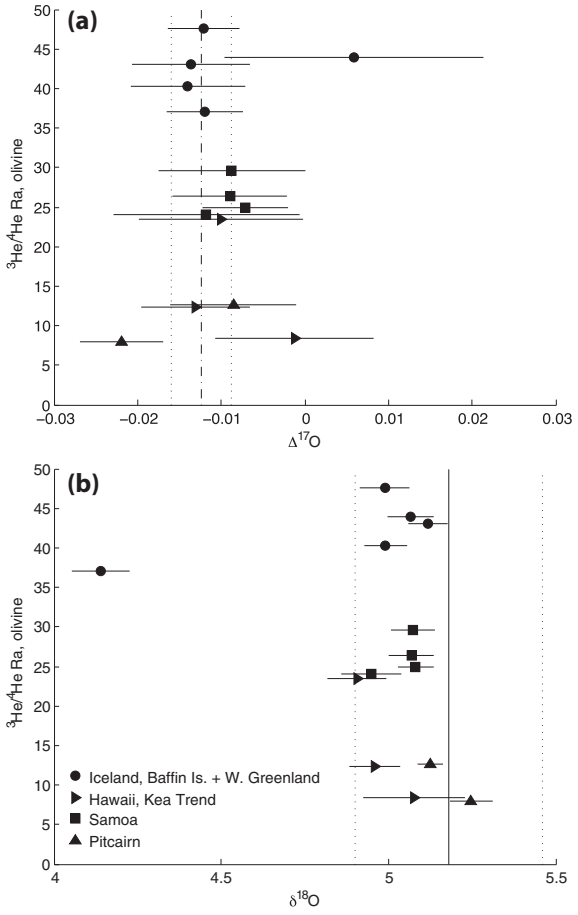

Fig. 1. New $\Delta^{17}O$ and $\delta^{18}O$ measurements on olivine with variable $^3He/^4He$ ratios. (a) $\Delta^{17}O$ values plotted as a function of $^3He/^4He$ ratio. $^3He/^4He$ ratios range up to 47.6 Ra but associated $\Delta^{17}O$ values from a variety of locations show no deviation from the bulk mantle mean $\Delta^{17}O$ value, as defined by replicate analyses of San Carlos olivine. Sample error bars are 2σ SEM. (b) $\delta^{18}O$ values plotted as a function of $^3He/^4He$ ratio. High-$^3He/^4He$ olivines have a narrow range of $\delta^{18}O$ values that are shifted to a lower value compared to mantle olivine mean (Mattey et al., 1994). Sample error bars are 2σ SEM. On (a) the bulk mantle (San Carlos) $\Delta^{17}O$ is defined by a dash-dot line. On (b) the bulk mantle $\delta^{18}O$ (Mattey et al., 1994) is defined by a solid line. In both diagrams 2σ errors are given by dotted lines.

High-$^3He/^4He$ olivines are defined here as samples with >20 Ra, >4.75 $\delta^{18}O$, and show no indications of crustal contamination (Table 1) and display a narrow range of $\delta^{18}O$ values (Fig. 1b). If olivines with an Ra value of <20, $\delta^{18}O < 4.75$‰ (SK1), and indications of crustal contamination (BI/CS/7) are excluded, our remaining 74 analyses of high-$^3He/^4He$ olivines have a mean $\delta^{18}O$ value of 5.017 (±0.016)‰ (Table 1). The average $\delta^{18}O$ value of the average mantle and high-$^3He/^4He$ olivines are significantly different (2-sample T-test p value = 0.002). The samples in the high-$^3He/^4He$ group cover nearly the entire range of

locations in this study, including Iceland, BI-WG, Samoa and Hawaii. The Icelandic sample (SK1) is noted to display particularly low $\delta^{18}O$, a feature which has previously been discussed by Macpherson et al. (2005) and is explained by interaction of the Icelandic melts with high-latitude, low $\delta^{18}O$ meteoric water. Sample BI/CS/7 is also suggested to be affected by crustal contamination (Starkey et al., 2009). As such, these samples do not likely represent a primary melt of their mantle source and are excluded from calculations related to the composition of the high-$^3He/^4He$ reservoir (Table 1).

Coupled $^3He/^4He$-$\delta^{18}O$ measurements on olivine (this study and published data, see Supplementary information for references) from a range of geographic/geochemical affinities (Iceland, Hawaii, Pitcairn, Samoa, HIMU-affinity, and "other") are presented in Fig. 2 to further explore the He–O isotope systematics. We use the term HIMU-affinity because many of the locations with coupled He–O–Pb isotopic measurements have elevated $^{206}Pb/^{204}Pb$ values but do not approach the global endmember. The highest $^3He/^4He$ olivines from a variety of geographic/geochemical affinities have a narrow range of $\delta^{18}O$ values, despite a wide range of $\delta^{18}O$ values observed for lower $^3He/^4He$ olivines. This convergence of $\delta^{18}O$ values at high $^3He/^4He$ is observed both within individual geographic/geochemical affinities (Iceland and Hawaii, Fig. 2a and b) and in the global compilation (Fig. 2g). There is evidence for a small $\delta^{18}O$ displacement of high-$^3He/^4He$ olivines to values lower than mean mantle olivine (solid vertical lines, Fig. 2, Mattey et al., 1994). The distinction between high-$^3He/^4He$ materials (olivines and olivine equivalent glasses, >20 Ra and >4.75 $\delta^{18}O$, this study and published data) and mean mantle olivine is also statistically significant (2-sample T-test p value = 0.00003). However, this result should be treated with some caution because of potential interlaboratory issues and the variability of San Carlos olivine as a reference material.

4. DISCUSSION

4.1. Transfer of oxygen from high-$^3He/^4He$ mantle source to high-$^3He/^4He$ magmatic olivine

Magmatic $^3He/^4He$ signatures are commonly quantified by measuring the composition of He released from olivine-hosted inclusions during crushing, while corresponding O isotopic compositions of olivines are measured on the bulk grain. Because the He and O measurements are not from the exact same material (inclusions vs. bulk olivine), and because He and O have variable sensitivity to crustal contamination and mixing, it is not required that high-$^3He/^4He$ olivines contain significant quantities of O derived from the high-$^3He/^4He$ mantle source. If true, O isotopic values would be essentially decoupled from $^3He/^4He$ values and provide little information regarding the nature of the high $^3He/^4He$ source.

Several lines of evidence argue that O and He remain coupled through magma genesis and melt migration processes. Despite the tendency for olivine to trap magmatic He and O relatively early in the crystallisation process, it is possible that He and O in a primary melt are principally derived from two unrelated mantle sources. Helium is highly incompatible in upper mantle solids (Heber et al., 2007; Jackson et al., 2013) and is correspondingly concentrated in small degree mantle melts. These small degree melts can migrate from their source and hyperbolically mix with other mantle materials. In this mixing scenario, the He isotopic composition of the resulting material will be dominated by the incompatible element-enriched, low degree melt, while the major element composition of the material will be dominated by the volumetrically major mixing component. If He is decoupled from less incompatible elements through low degree melts or other hyperbolic mixing processes, it is expected that high-$^3He/^4He$ materials will have highly variable Sr, Nd, Pb, and O isotopic compositions. Whereas, if He remains coupled to less incompatible elements through melt production and migration processes, it is expected that high-$^3He/^4He$ materials from a given location will cluster in a restricted range of Sr, Nd, Pb, and O isotopic space. Broad correlations between $^3He/^4He$ and radiogenic isotope values ($^{87}Sr/^{86}Sr$, $\varepsilon^{143}Nd$, $^{206}Pb/^{204}Pb$) have previously been identified (Hart et al., 1992, Supplementary information), although this relationship does not always hold within specific regional groups (e.g., BI-WG, Starkey et al., 2009, 2012). However, the fact that high-$^3He/^4He$ olivine from a wide variety of geographic/geochemical affinities share similar $\delta^{18}O$ values, and that $^3He/^4He$ variability is often correlated with $\delta^{18}O$ variability (Fig. 2), argues for the coupling of He and O during melt production and migration processes. This, in turn, implies that O contained within a high-$^3He/^4He$ olivine is dominantly sourced from a high-$^3He/^4He$ mantle source. We also note that BI-WG samples were screened on the basis of trace element chemistry to be free of crustal contamination (Starkey et al., 2009), further supporting the connection of our measured $\delta^{18}O$ values to their mantle source value.

4.2. $\Delta^{17}O$ composition of high-$^3He/^4He$ olivine

The main observation of this study is that the $\Delta^{17}O$ composition of high-$^3He/^4He$ olivines is indistinguishable from the $\Delta^{17}O$ composition of the bulk mantle to high precision, where the bulk mantle $\Delta^{17}O$ value is defined by San Carlos olivine (Table 1). This suggests that post-accretion processes have effectively homogenised primordial major element heterogeneities, or that such heterogeneities were small or non-existent to begin with (e.g., Dauphas et al., 2014; Mastrobuono-Battisti et al., 2015). This result is consistent with previous attempts to detect $\Delta^{17}O$ anomalies in Precambrian rocks relative to modern rocks (Robert et al., 1992; Rumble et al., 2013).

There are a number of scenarios that could account for homogenous $\Delta^{17}O$ values throughout the solid Earth. Scenario 1 is that the Earth underwent homogenous O isotope accretion, resulting in no difference between the $\Delta^{17}O$ composition for early-formed mantle reservoirs and bulk mantle. Although our results are consistent with such a model, this model is not supported by the range of O isotope compositions measured in the inner solar system

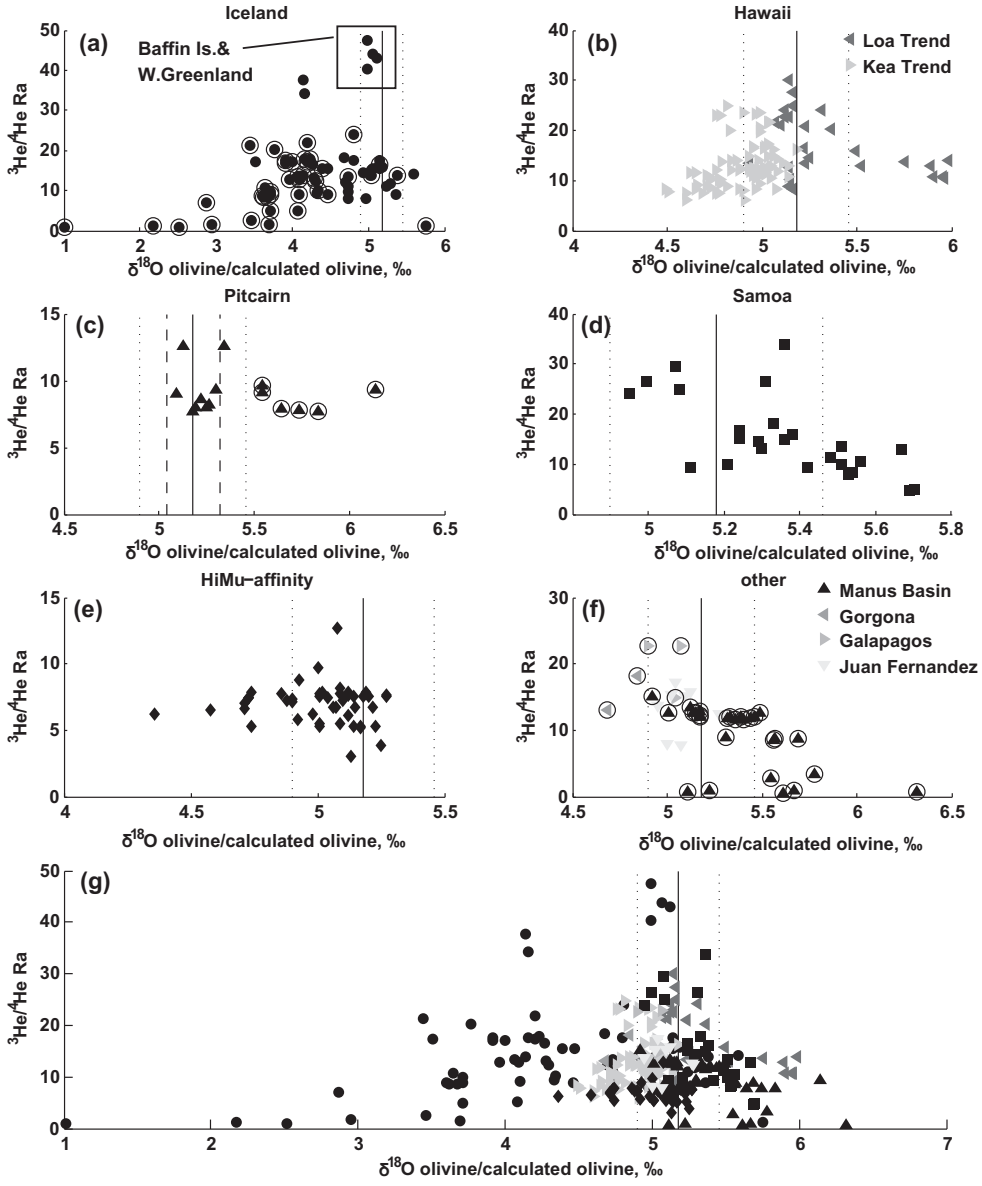

Fig. 2. $^{3}He/^{4}He$-$\delta^{18}O$ measurements plotted by (a–f) geographic/geochemical affinities and (g) as a global compilation. The highest $^{3}He/^{4}He$ olivines with a variety of geographic/geochemical affinities have a narrow range of $\delta^{18}O$ values, despite a wide range of $\delta^{18}O$ values observed for lower $^{3}He/^{4}He$ olivine. This suggests He and O remain coupled during melt production and migration processes (see Section 4.1). Data points with surrounding circles have been converted to $\delta^{18}O$-olivine equivalent values using the mineral–mineral fractionations from Mattey et al. (1994) for clinopyroxene and Eiler et al. (2000a) for glass and plagioclase. All conversions are from glass to olivine except from the Gorgona and Galapagos data.

(Clayton, 1993; Franchi, 2008) and our current dynamical understanding of accretion (Kaib and Cowan, 2015). Thus, it seems unlikely that the Earth would have accreted homogenously in terms of O isotopes, a concept which is supported by Herwartz et al. (2014).

On the other hand, the data obtained in this study can be used to test a number of heterogeneous O isotope accretion possibilities. Scenario 2 involves isolation of the high-$^{3}He/^{4}He$ source prior to the cessation of accretion (i.e., prior to the Moon-forming impact) followed by later extensive homogenisation between it and the bulk mantle. Scenario 3 involves isolation of the high-$^{3}He/^{4}He$ source following the end of accretion and homogenisation of Earth (after the last significant shift of bulk mantle $\Delta^{17}O$ – i.e., after the Moon-forming impact, or potentially the late veneer). As it is not clear exactly what process formed the high-$^{3}He/^{4}He$ reservoir, in these models we use 'isolation' in general terms to describe the early chemical isolation of high-$^{3}He/^{4}He$ mantle, as required by short-lived Xe isotopic measurements (Mukhopadhyay, 2012; Peto et al., 2013) and suggested by short-lived W isotopic measurements (Touboul et al., 2012).

Here we introduce a two-stage mixing model in support of Scenario 2. The standard model for the formation of the

Moon has a Mars-sized impactor (10% of Earth's current mass) colliding with the Earth (Canup, 2004). Mixing of a Moon-forming impactor with the bulk mantle would result in an intermediate $\Delta^{17}O$ composition that is determined by the relative masses and initial $\Delta^{17}O$ values of these two end-members. For example, if the bulk mantle was 85% of the present silicate Earth and equilibrated with a Mars-sized impactor (10% of present Earth mass) with Mars-like $\Delta^{17}O$ ($\Delta^{17}O_{Mars} = 0.301‰$, Franchi et al., 1999), the resultant mixture would have a $\Delta^{17}O$ composition that is increased by 0.032‰. In this calculation, high-$^3He/^4He$ mantle occupies the remaining 5% of silicate Earth, and if not involved in the homogenisation with the impactor, would still have a $\Delta^{17}O$ value that is 0.032‰ lower than the bulk mantle. This difference in $\Delta^{17}O$ between the bulk mantle and the high-$^3He/^4He$ mantle is large and not observed given the present data, allowing this mixing scenario to be rejected.

An initially different $\Delta^{17}O$ composition for high-$^3He/^4He$ mantle, however, could be obscured if there was later exchange of materials between bulk mantle and high-$^3He/^4He$ mantle (i.e., a two-stage mixing model, Fig. 3). Modelling the exchange as an equal-mass process (no change in mass for either reservoir), homogenisation of the high-$^3He/^4He$ reservoir and bulk mantle must progress to at least 90%, given a limit of +0.002/−0.004‰ (2 SEM) for the difference in $\Delta^{17}O$ between the bulk mantle and high-$^3He/^4He$ mantle (Fig. 3). This same exchange results in a 0.001‰ decrease of $\Delta^{17}O$ for the bulk mantle. A change of 0.003‰ is the maximum allowable $\Delta^{17}O$ shift for bulk Earth, taking the Moon as a proxy for the initial O isotope composition of bulk Earth and the $\Delta^{17}O$ measurement of the Earth–Moon difference as calculated by Wiechert et al. (2001) (2 SEM), a difference which is in agreement with Hallis et al. (2010). Thus, this scenario can satisfy the available $\Delta^{17}O$ constraints for the Earth–Moon-high-$^3He/^4He$ mantle system and cannot be rejected. However, it should be noted that there is some disagreement in the recent literature over the Earth–Moon difference, with one study (Herwartz et al., 2014) detecting a larger difference than that used in this modelling. This possibility is discussed below. By taking the Moon as a proxy for the initial O isotope composition of bulk Earth, we make the implicit assumption that oxygen was highly homogenised between these two bodies in the aftermath of the impact event.

Using the constraints provided by the similarity of $\Delta^{17}O$ in the Earth–Moon-high-$^3He/^4He$ reservoir system, we can determine permissible parameters for the mass of the high-$^3He/^4He$ reservoir, mass of the Moon-forming impactor, and the $\Delta^{17}O$ difference between the impactor and Earth (Fig. 3). These scenarios follow the same form as outlined in the example provided above.

For all these models, some degree of homogenisation of the high-$^3He/^4He$ reservoir and bulk mantle is needed to account for the similarity of their $\Delta^{17}O$ compositions, i.e., high-$^3He/^4He$ is not a closed system and cannot be regarded as strictly primordial at the major element level. For mixing calculations focused on exploring the effect of impactor $\Delta^{17}O$ composition (Fig. 3a) we adopt the more canonical approach of assuming a Mars-sized impactor (10% of present Earth, with a mantle/core mass ratio equal to present-day Earth) and assume the size of the high-$^3He/^4He$ reservoir to be 5% of the present-day mantle. If we take the $\Delta^{17}O$ composition of the impactor to be ±0.15‰ (i.e., the "mean $\Delta^{17}O$" difference between bulk mantle and giant impactors, as calculated by Pahlevan and Stevenson (2007)) then this scenario requires >60% homogenisation of the high-$^3He/^4He$ reservoir and bulk mantle to mute the difference in $\Delta^{17}O$ imparted between these reservoirs following the Moon-forming impact (Fig. 3a). In the case of extremely similar, or extremely different, $\Delta^{17}O$ values for bulk mantle$_i$ and the impactor, (i.e., an angrite-like or Mars-like impactor), >20% and >90%

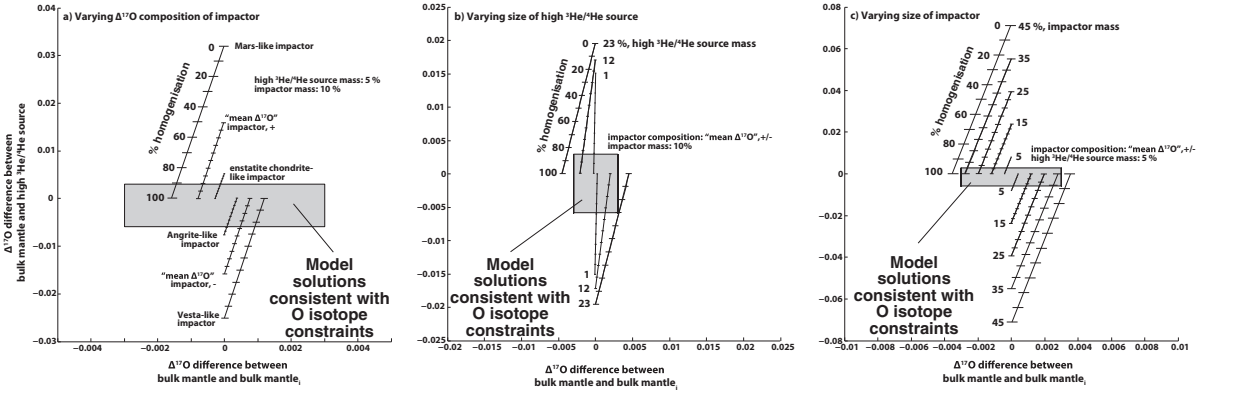

Fig. 3. $\Delta^{17}O$ mixing models between the bulk mantle and an early isolated high-$^3He/^4He$ source. The *y*-axes plot the $\Delta^{17}O$ difference between the bulk mantle and high-$^3He/^4He$ source as a function of homogenisation percentage. The *x*-axes plot the $\Delta^{17}O$ difference between bulk mantle and bulk mantle$_i$ as a function of homogenisation percentage. Bulk mantle$_i$ denotes the bulk mantle after mixing with the Moon-forming impactor but prior to any homogenization with the high-$^3He/^4He$ source. Horizontal tick marks along a given mixing line represents a 10% increment of homogenisation. Horizontal solid lines of the grey box represent the maximum $\Delta^{17}O$ difference between the bulk mantle and high $^3He/^4He$ source (2σ, SEM). Vertical solid lines of the grey box represent the maximum $\Delta^{17}O$ difference between the Moon and Earth (2σ, SEM; Wiechert et al., 2001). Panel (a) displays the mixing systematics for impactors with different $\Delta^{17}O$ values. Panel (b) displays the mixing systematics for scenarios with different mass high-$^3He/^4He$ source reservoirs. Panel (c) displays the mixing systematics for scenarios with different mass impactors.

homogenisation, respectively, are required for the scenario parameters. The angrite-like and Mars-like impactor compositions are taken from Greenwood et al. (2005) and Franchi et al. (1999), respectively. Changing the mass of the high-^{3}He/^{4}He reservoir does not substantially affect the percentage of homogenisation required, holding other variables constant (Fig. 3b). For an impactor with a "mean Δ^{17}O" composition, increasing the volume of the high-^{3}He/^{4}He reservoir from 1% to 40% of the mantle results in the homogenisation requirement changing from >60% to >75%.

Scenarios with impactors smaller than the canonical size require less homogenisation. Reducing the impactor mass from 10% to 5% of present Earth mass effectively halves the required amount of homogenisation (Fig. 3c). Larger impactors require increasing amounts of homogenisation for a given O isotope composition. If an impactor with "mean Δ^{17}O" exceeds 40% of the present Earth mass, homogenisation of the high-^{3}He/^{4}He reservoir (5% of present-day mantle mass) and bulk mantle generates a corresponding Δ^{17}O shift in the bulk mantle that is larger than the difference between the Earth and Moon as calculated by Wiechert et al. (2001) and Hallis et al. (2010), but smaller than the difference as calculated by Herwartz et al. (2014) (solid vertical lines, Wiechert et al., 2001, Fig. 3). Similarly, if the high-^{3}He/^{4}He reservoir exceeds (or previously exceeded) 20% of the present-day mantle mass, homogenisation of the high-^{3}He/^{4}He reservoir and the bulk mantle generates corresponding Δ^{17}O shifts in the bulk mantle that are larger than the current difference between the Earth and Moon (vertical solid lines, Fig. 3b). Taking this scenario, homogenisation during the giant impact phase of Earth's accretion appears to involve a large majority of the mantle, including both the upper mantle and majority of the lower mantle. This conclusion is dependent on the assumed Δ^{17}O composition and size of the impactor. Smaller impactors, and with less distinct Δ^{17}O compositions, allow for more of the mantle to have remained isolated.

It is worth noting that recent measurements of Δ^{17}O for Moon and Earth materials yield a difference of +0.012 ± 0.006‰ (Herwartz et al., 2014), in disagreement with previous determinations (Wiechert et al., 2001; Hallis et al., 2010). If these newer measurements are robust, the lunar Δ^{17}O composition no longer constrains the Δ^{17}O composition of bulk mantle$_i$ to a specific value. Rather, a high lunar Δ^{17}O value would suggest the impactor also had a relatively high Δ^{17}O value. Following this, the terrestrial bulk mantle would have a relatively high Δ^{17}O value compared to any early isolated reservoir. This potential scenario allows us to only consider the upper bound of the high-^{3}He/^{4}He reservoir Δ^{17}O constraint (upper edge of grey boxes, Fig. 4), which is tighter than the lower bound. Only considering this upper bound, an impact scenario with an enstatite chondrite-like impactor (composition from Herwartz et al., 2014), which represents an impactor with an extremely similar Δ^{17}O value to bulk mantle$_i$, still requires >40% homogenisation (Fig. 3b). A small, positive Δ^{17}O difference between the Moon and Earth also requires that the formation of the Moon acted to shift Δ^{17}O of the bulk mantle and that any early isolated reservoir, i.e., the high-^{3}He/^{4}He

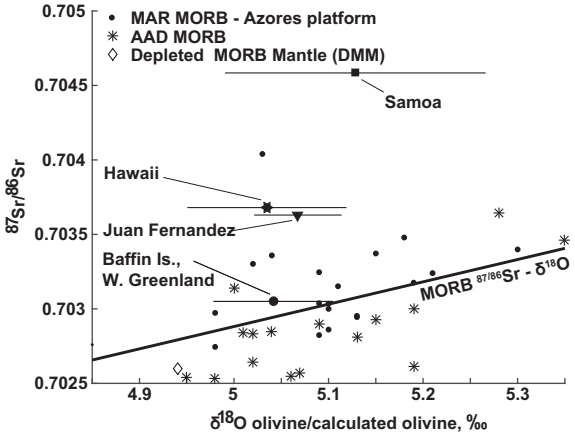

Fig. 4. ^{87}Sr/^{86}Sr and δ^{18}O systematics of MORB and high-^{3}He/^{4}He mantle locations. In the MORB data set, ^{87}Sr/^{86}Sr and δ^{18}O positively correlate, while ^{87}Sr/^{86}Sr and δ^{18}O are not correlated between different high-^{3}He/^{4}He mantle locations. The δ^{18}O composition of high-^{3}He/^{4}He mantle locations is determined by averaging the δ^{18}O values of the highest ^{3}He/^{4}He samples associated with that location (>40 Ra for Iceland, >20 Ra for Hawaii, >20 Ra for Samoa, >15 Ra for Juan Fernandez). Sr isotope compositions are from Jackson et al. (2007) for Hawaii, Samoa and Juan Fernandez, Stuart et al. (2003) for Iceland and Starkey et al. (2009) for BI-WG. All MORB data have been converted to $\delta^{18}O_{olivine}$ equivalent. The DMM point is generated using the corresponding δ^{18}O value from Cooper et al., 2004 and ^{87}Sr/^{86}Sr value from Salters and Stracke (2004).

mantle, should have a relatively low Δ^{17}O value, supporting the mixture modelling presented above.

In Scenario 3 we look at the possibility that the homogeneity of Δ^{17}O in the solid Earth can be explained by isolation of the high-^{3}He/^{4}He mantle following the last addition of cosmochemically distinctive oxygen to Earth (i.e., after the Moon-forming impact). The time-window for this possibility is narrow, i.e., >50 Ma after, but <80 Ma after CAIs. This window is based on the likelihood that (1) the Moon-forming impact was associated with the delivery of anomalous O (as indicated by Herwartz et al. (2014) and analyses of other inner solar system materials) and occurred after the lifetime of ^{182}Hf (i.e., >50 Ma after CAI; Touboul et al., 2007), and (2) the high-^{3}He/^{4}He reservoir was isolated within the lifetime of ^{129}I (i.e., <80 Ma after CAI; Mukhopadhyay, 2012; Peto et al., 2013). In light of the evidence for Moon formation >100 Ma after CAI condensation (Nemchin et al., 2009; Nyquist et al., 2010; McLeod et al., 2014 and references within), and for the association of plumes with high ^{3}He/^{4}He and anomalous ^{182}W/^{184}W ratios (Touboul et al., 2012), we consider it more likely that high-^{3}He/^{4}He mantle was isolated prior to the end of Earth's accretion (taken here to mean the giant Moon-forming impact) and that subsequent interactions with the bulk mantle have effectively obscured any distinctions in Δ^{17}O (Scenario 2). It is also possible that the late veneer shifted the bulk mantle Δ^{17}O composition as much as 0.020‰ (Herwartz et al., 2014). This exceeds the precision of the current study, also supporting Scenario 2.

A principal contention of Scenario 2 is that high-^{3}He/^{4}He mantle is not a pristine primordial reservoir. Rather, it is an early-forming reservoir that has experienced subsequent homogenisation with bulk mantle materials and that the degree of this homogenisation can be constrained using mixing models (Fig. 3). The possibility that high-^{3}He/^{4}He mantle is not a pristine primordial reservoir is supported by recent arguments for extensive amounts of recycling of modern atmospheric Xe into the high-^{3}He/^{4}He reservoir (~85% of total Xe in mantle source; Mukhopadhyay, 2012; Peto et al., 2013) and the differences in radiogenic isotopic composition observed between high-^{3}He/^{4}He locations globally (Jackson et al., 2007, Supplementary information). Thus, our findings add to the evidence for an open-system, high-^{3}He/^{4}He mantle source that is also robust to complete mixing over nearly the entirety of Earth's history. If the high-^{3}He/^{4}He mantle source is related to lower mantle structure (e.g., large low shear velocity provinces or ultra-low velocity zones), our findings also imply that these structures are not strictly primordial, rather they represent a combination of both early-forming materials and materials sourced from the Earth's lithosphere. This possibility gains support from recent dynamical modelling efforts focused on understanding the interactions between large low shear velocity provinces and recycled materials (Li et al., 2014).

4.3. Implications for the δ^{18}O values of high-^{3}He/^{4}He olivines

High-^{3}He/^{4}He olivines from a wide variety of locations appear to have a common δ^{18}O composition near 5‰ (Fig. 2). Mass dependent O isotope variability can result from melting-crystallisation processes, source variations, and near-surface contamination. Samoa and Hawaii are located on top of thick lithosphere, which acts to truncate their melting column, concentrating lower degree melts from higher pressure and temperature regimes. The modern Iceland plume is associated with a rifting environment which promotes higher degree melts from lower pressure and temperature regimes. BI-WG are also associated with a rifting environment but here the proto-Iceland plume impacted a thick lithospheric lid (~100 km). The fact that the highest ^{3}He/^{4}He olivines from a variety of tectonic settings have consistent δ^{18}O values suggests that melting/crystallisation processes and near-surface contamination are not dominant factors in determining the δ^{18}O of these samples. Given this, we interpret the measured δ^{18}O values of high-^{3}He/^{4}He olivine as representative of their mantle source, although analyses of a wider range of samples from a single laboratory are needed to confirm this.

Variations of δ^{18}O in multiple MORB glass datasets are positively correlated with indices of geochemical enrichment (Eiler et al., 2000b; Cooper et al., 2004, 2009; Fig. 4). This suggests two things regarding the MORB mantle source: (1) the depleted MORB mantle (DMM, MORB mantle without the recycled components; diamond symbols in Fig. 4, O from Cooper et al., 2004, Sr from Salters and Stracke, 2004) has a δ^{18}O composition that is lower than the mean mantle and (2) materials with relatively high δ^{18}O values are the dominant source of δ^{18}O variability in the convecting mantle. Fig. 4 also shows the correlation of ^{87}Sr/^{86}Sr and δ^{18}O values for high-^{3}He/^{4}He materials (O data from Eiler et al., 1997; Workman et al., 2008; this study). High-^{3}He/^{4}He mantle likely has a higher concentration of Sr compared to DMM but an essentially equal concentration of O. Given this, if δ^{18}O variations of high-^{3}He/^{4}He mantle are controlled by the same materials that dominate δ^{18}O variations in the MORB source, we would expect a correlation between ^{87}Sr/^{86}Sr and δ^{18}O values that is less steep than the MORB correlation. This is not observed (Fig. 4), suggesting that δ^{18}O variability in the MORB source and high-^{3}He/^{4}He mantle are controlled by distinct materials.

The correlation between δ^{18}O and ^{87}Sr/^{86}Sr in MORB is interpreted to result from mixing between DMM and recycled pelagic sediment (Eiler et al., 2000b; Cooper et al., 2009). The lack of δ^{18}O-^{87}Sr/^{86}Sr covariation in high-^{3}He/^{4}He samples implies that pelagic sediment, or any other high δ^{18}O recycled component, is not the volumetrically dominant material recycled into high-^{3}He/^{4}He mantle. Rather, the relative uniformity of δ^{18}O values suggests that any components recycled into the high-^{3}He/^{4}He reservoir have δ^{18}O values that, when averaged, are similar to the DMM. HIMU (high-U/Pb)-affinity materials have δ^{18}O compositions similar to DMM or slightly higher than DMM (Eiler et al., 1997; Day et al., 2014; Supplementary material), while EM1 (Samoan Rejuvenated Component, and Koolau Component) and EM2 (Samoan Malu Component) endmembers are associated with relatively high δ^{18}O values (Eiler et al., 1997; Fig. 2, Supplementary information). This observation, thus, points to a large role for HIMU-affinity materials or another recycled component with a δ^{18}O similar to DMM, in explaining the open-system behaviour of high-^{3}He/^{4}He mantle (Albarede, 1998; Class and Goldstein, 2005; Garapic et al., 2015).

Global endmember HIMU materials do not have radiogenic ^{87}Sr/^{86}Sr values and cannot explain the ^{87}Sr/^{86}Sr variation observed between the high-^{3}He/^{4}He components expressed at different plume locations (Fig. 4). HIMU-like signatures are commonly observed within both MORB and OIB that have relatively radiogenic ^{87}Sr/^{86}Sr values but more moderate ^{206}Pb/^{204}Pb values (Stracke et al., 2005). Given the ubiquity of this material throughout the mantle, it has been suggested that it represents a component that is internal to the mantle tetrahedron, i.e., a HIMU-affinity FOZO, possibility related to recycled oceanic crust that is less modified by subduction compared to global endmember HIMU. This HIMU-affinity component is able to explain the δ^{18}O–^{87}Sr/^{86}Sr variations between high-^{3}He/^{4}He components.

5. CONCLUSIONS

The mean Δ^{17}O composition of olivines from non-crustally contaminated, high-^{3}He/^{4}He (>20 Ra, δ^{18}O > 4.75‰) OIB is indistinguishable from mean mantle olivine to high precision, despite evidence for the early isolation of high-^{3}He/^{4}He mantle. We introduce 3 scenarios that can account for the similarity in Δ^{17}O of the solid Earth: (1) homogenous O isotope accretion, (2) isolation

of the high-^{3}He/^{4}He source prior to the cessation of accretion and later extensive homogenisation between it and the bulk mantle or (3) isolation of the high-^{3}He/^{4}He source after the last significant shift of Δ^{17}O in the bulk mantle. Scenario (2) is favoured, but regardless of which possibility correctly explains the homogeneity of Δ^{17}O throughout the solid Earth, the results indicate that, to high precision, there is no evidence that the Earth contains cosmochemically distinct reservoirs for major elements.

Olivines with high-^{3}He/^{4}He values extracted from plume lavas have mean δ^{18}O of ~5‰. The fact that there is a narrow range of δ^{18}O values associated with high-^{3}He/^{4}He olivines, and that, globally, there are correlations between δ^{18}O and radiogenic isotopes (He, Nd, Sr, and Nd; see Fig. 2 and Supplementary information) implies that O remains coupled to the more incompatible elements during melt production and migration processes. The δ^{18}O value for high-^{3}He/^{4}He materials may suggest that moderate δ^{18}O materials (e.g., HIMU-affinity materials) are the dominant recycling components for high-^{3}He/^{4}He mantle.

ACKNOWLEDGEMENTS

The authors would like to thank the following people for providing samples and/or helpful discussions during the course of this project and manuscript preparation: Colin Macpherson, Zhengrong Wang, Stan Hart, Alberto Saal and Nathan Kaib. We would like to thank Jenny Gibson for assistance with the oxygen isotope analyses. Oxygen isotope work at the Open University is funded by a consolidated grant from STFC.

APPENDIX A. SUPPLEMENTARY DATA

Supplementary data associated with this article can be found, in the online version, at http://dx.doi.org/10.1016/j.gca.2015.12.027.

REFERENCES

Albarede F. (1998) Time-dependent models of U–Th–He and K–Ar evolution and the layering of mantle convection. *Chem. Geol.* **145**, 413–429.

Bryce J. G., DePaolo D. J. and Lassiter J. C. (2005) Geochemical structure of the Hawaiian plume: Sr, Nd, and Os isotopes in the 2.8 km HSDP-2 section of Mauna Kea volcano. *Geochem. Geophys. Geosyst.* **6**. http://dx.doi.org/10.1029/2004GC000809, Q09G18.

Canup R. M. (2004) Simulations of a later lunar-forming impact. *Icarus* **168**, 433–456.

Chambers J. (2001) Making more terrestrial planets. *Icarus* **152**, 205–224.

Class C. and Goldstein S. L. (2005) Evolution of helium isotopes in the Earth's mantle. *Nature* **436**, 1107–1112.

Clayton R. N. (1993) Oxygen isotopes in meteorites. *Annu. Rev. Earth Planet. Sci.* **21**, 115–149.

Cooper K. M., Eiler J. M., Asimow P. D. and Langmuir C. H. (2004) Oxygen-isotope evidence for the origin of enriched mantle beneath the mid-Atlantic ridge. *Earth Planet. Sci. Lett.* **220**, 297–316.

Cooper K. M., Eiler J. M., Sims K. W. W. and Langmuir C. H. (2009) Distribution of recycled crust within the upper mantle: insights from the oxygen isotope composition of MORB from the Australian-Antarctic discordance. *Geochem. Geophys. Geosyst.* **10**, Q12004. http://dx.doi.org/10.1029/2009GC002728.

Dauphas N., Burkhardt C., Warren P. H. and Fang-Zhen T. (2014) Geochemical arguments for an Earth-like Moon-forming impactor. *Philos. Trans. R. Soc. London, Ser. A* **372**, 20130244.

Day J., Peters B. J. and Janney P. E. (2014) Oxygen isotope systematics of South African olivine melilites and implications for HIMU mantle reservoirs. *Lithos* **202–203**, 76–84.

Eiler J. M., Farley K. A., Valley J. W., Hauri E., Craig H., Hart S. R. and Stolper E. M. (1997) Oxygen isotope variations in ocean island basalt phenocrysts. *Geochim. Cosmochim. Acta* **61**, 2281–2293.

Eiler J. M., Crawford A., Elliott T. I. M., Farley K. A., Valley J. W. and Stolper E. M. (2000a) Oxygen isotope geochemistry of oceanic-arc lavas. *J. Petrol.* **41**, 229–256.

Eiler J. M., Schiano P., Kitchen N. and Stolper E. M. (2000b) Oxygen-isotope evidence for recycled crust in the sources of mid-ocean-ridge basalts. *Nature* **403**, 530–534.

Ellam R. M. and Stuart F. M. (2004) Coherent He–Nd–Sr isotope trends in high ^{3}He/^{4}He basalts: implications for a common reservoir, mantle heterogeneity and convection. *Earth Planet. Sci. Lett.* **228**, 511–523.

Franchi I. A. (2008) Oxygen isotopes in asteroidal materials. *Rev. Mineral.* **68**, 345–397.

Franchi I. A., Wright I. P., Sexton A. S. and Pillinger C. T. (1999) The oxygen-isotopic composition of Earth and Mars. *Meteorit. Planet. Sci.* **34**, 657–661.

Garapic G., Jackson M. G., Hauri E. H., Hart S. R., Farley K. A., Blusztajn J. S. and Woodhead J. D. (2015) A radiogenic isotopic (He–Sr–Nd–Pb–Os) study of lavas from the Pitcairn hotspot: implications for the origin of EM-1 (enriched mantle 1). *Lithos* **228–229**, 1–11.

Greenwood R. C., Franchi I. A., Jambon A. and Buchanan P. C. (2005) Widespread magma oceans on asteroidal bodies in the early solar system. *Nature* **435**, 916–918.

Hallis L., Anand M., Greenwood R. C., Miller M. F., Franchi I. A. and Russell S. (2010) The oxygen isotope composition, petrology and geochemistry of mare basalts: evidence for large-scale compositional variation in the lunar mantle. *Geochim. Cosmochim. Acta* **74**, 6885–6899.

Hart S., Hauri E., Oschmann L. and Whitehead J. (1992) Mantle plumes and entrainment: isotopic evidence. *Science* **256**, 517–520.

Heber V. S., Brooker R. A., Kelley S. P. and Wood B. J. (2007) Crystal-melt partitioning of noble gases (helium, neon, argon, krypton, and xenon) for olivine and clinopyroxene. *Geochim. Cosmochim. Acta* **71**, 1041–1061.

Herwartz D., Pack A., Friedrichs B. and Bischoff A. (2014) Identification of the giant impactor Theia in lunar rocks. *Science* **344**, 1146–1150.

Jackson M. G., Kurz M. D., Hart S. R. and Workman R. K. (2007) New Samoan lavas from Ofu Island reveal a hemispherically heterogeneous high ^{3}He/^{4}He mantle. *Earth Planet. Sci. Lett.* **264**, 360–374.

Jackson C. R. M., Parman S. W., Kelley S. P. and Cooper R. F. (2013) Constraints on light noble gas partitioning at the conditions of spinel-peridotite melting. *Earth Planet. Sci. Lett.* **384**, 178–187.

Kaib N. A. and Cowan N. B. (2015) The feeding zones of terrestrial planets and insights in to Moon formation. *Icarus* **252**, 161–174.

Kurz M. D., Jenkins W. J. and Hart S. R. (1982) Helium isotopic systematics of oceanic islands and mantle heterogeneity. *Nature* **297**, 43–47.

Kurz M. D., Curtice J., Lott, III, D. E. and Solow A. (2004) Rapid helium isotopic variability in Mauna Kea shield lavas from the Hawaiian Scientific Drilling Project. *Geochem. Geophys. Geosyst.* **5**. http://dx.doi.org/10.1029/2002GC000439.

Kusakabe M. and Matsuhisa Y. (2008) Oxygen three-isotope ratios of silicate reference materials determined by direct comparison with VSMOW-oxygen. *Geochem. J.* **42**, 309–317.

Li Y., Deschamps F and Tackley P. J. (2014) Effects of low-viscosity post-perovskite on the stability and structure of primordial reservoirs in the lower mantle. *Geophys. Res. Lett.* **41**. http://dx.doi.org/10.1002/2014GL061362.

Macpherson C. G., Hilton D. R., Mattey D. P. and Sinton J. M. (2000) Evidence for an ^{18}O-depleted mantle plume from contrasting $^{18}O/^{16}O$ ratios of back-arc lavas from the Manus Basin and Mariana Trough. *Earth Planet. Sci. Lett.* **176**, 171–183.

Macpherson C. G., Hilton D. R., Day J. M. D., Lowry D. and Gronvold K. (2005) High-$^3He/^4He$, depleted mantle and low-$\delta^{18}O$, recycled oceanic lithosphere in the source of central Iceland magmatism. *Earth Planet. Sci. Lett.* **233**, 411–427.

Mastrobuono-Battisti A., Perets H. B. and Raymond S. N. (2015) A primordial origin for the compositional similarity between the Earth and the Moon. *Nature* **520**, 212–215.

Mattey D. and Macpherson C. (1993) High precision oxygen isotope microanalysis of ferromagnesian minerals by laser-fluorination. *Chem. Geol.* **105**, 305–318.

Mattey D., Lowry D. and Macpherson C. (1994) Oxygen isotope composition of mantle peridotite. *Earth Planet. Sci. Lett.* **128**, 231–241.

McKeegan K. D., Kallio A. P. A., Heber V. S., Jarzebinski G., Mao P. H., Coath C. D., Kunihiro T., Wiens R. C., Nordholt J. E., Moses R. W., Reisenfeld D. B., Jurewicz A. J. G. and Burnett D. S. (2011) The oxygen isotopic composition of the Sun inferred from captured solar wind. *Science* **332**, 1528–1532.

McLeod C. L., Brandon A. D. and Armytage R. M. (2014) Constraints on the formation age and evolution of the Moon from ^{142}Nd–^{143}Nd systematics of Apollo 12 basalts. *Earth Planet. Sci. Lett.* **396**, 179–189.

Miller M. F. (2002) Isotopic fractionation and quantification of ^{17}O anomalies in the oxygen three-isotope system: an appraisal and geochemical significance. *Geochim. Cosmochim. Acta* **66**, 1881–1889.

Miller M. F., Greenwood R. C. and Franchi I. A. (2015) Comment on "The triple oxygen isotope composition of the Earth mantle and understanding variations in terrestrial rocks and minerals" by Pack and Herwartz [Earth Planet. Sci. Lett. 390 (2014) 138–145]. *Earth Planet. Sci. Lett.* **418**, 181–183.

Miller M. F., Franchi I. A., Sexton A. S. and Pillinger C. T. (1999) High precision $\delta^{17}O$ measurements of oxygen from silicates and other oxides: method and applications. *Rapid Commun. Mass Spectrom.* **13**, 1211–1217.

Mukhopadhyay S. (2012) Early differentiation and volatile accretion recorded in deep-mantle neon and xenon. *Nature* **486**, 101–104.

Nakajima M. and Stevenson D. J. (2015) Melting and mixing states of the Earth's mantle after the Moon-forming impact. *Earth Planet. Sci. Lett.* **427**, 286–295.

Nemchin A., Timms N., Pidgeon R., Geisler T., Reddy S. and Meyer C. (2009) Timing of crystallization of the lunar magma ocean constrained by the oldest zircon. *Nat. Geosci.* **2**, 133–136.

Nyquist L. E., Shih C.-Y., Reese D., Park J., Garrison D. and Yamaguchi A. (2010) Lunar crustal history recorded in lunar anorthosites. *Lunar Planet. Sci. Conf.* **41**, 1383.

Pack A. and Herwartz D. (2014) The triple oxygen isotope composition of the Earth mantle and understanding variations in terrestrial rocks and minerals. *Earth Planet. Sci. Lett.* **390**, 138–145.

Pahlevan K. and Stevenson D. J. (2007) Equilibration in the aftermath of the lunar-forming giant impact. *Earth Planet. Sci. Lett.* **262**, 438–449.

Peto M. K., Mukhopadhyay S. and Kelley K. A. (2013) Heterogeneities from the first 100 million years recorded in deep mantle noble gases from the Northern Lau Back-arc Basin. *Earth Planet. Sci. Lett.* **369**, 13–23.

Robert F., Rejou-Michel A. and Javoy M. (1992) Oxygen isotopic homogeneity of the Earth: new evidence. *Earth Planet. Sci. Lett.* **108**, 1–9.

Rumble D., Bowring S., Iizuka T., Komiya T., Lepland A., Rosing M. and Ueno Y. (2013) The oxygen isotope composition of Earth's oldest rocks and evidence of a terrestrial magma ocean. *Geochem. Geophys. Geosyst.* **14**, 1929–1939.

Salters V. J. M. and Stracke A. (2004) Composition of the depleted mantle. *Geochem. Geophys. Geosyst.* **5**, Q05004.

Starkey N. A., Stuart F. M., Ellam R. M., Fitton J. G., Basu S. and Larsen L. M. (2009) Helium isotopes in early Iceland plume picrites: constraints on the composition of high $^3He/^4He$ mantle. *Earth Planet. Sci. Lett.* **277**, 91–100.

Starkey N. A., Fitton J. G., Stuart F. M. and Larsen L. M. (2012) Melt inclusions in olivines from early Iceland plume picrites support high $^3He/^4He$ in both enriched and depleted mantle. *Chem. Geol.* **306–307**, 54–62.

Stracke A., Hoffman A. W. and Hart S. R. (2005) FOZO, HIMU, and the rest of the mantle zoo. *Geochem. Geophys. Geosyst.* **6**, Q05007.

Stuart F. M., Lass-Evans S., Fitton J. G. and Ellam R. M. (2003) High $^3He/^4He$ ratios in picritic basalts from Baffin Island and the role of a mixed reservoir in mantle plumes. *Nature* **424**, 57–59.

Thirlwall M. F., Gee M. A. M., Lowry D., Mattey D. P., Murton B. J. and Taylor R. N. (2006) Low ^{18}O in the Icelandic mantle and its origins: evidence from Reykjanes Ridge and Icelandic lavas. *Geochim. Cosmochim. Acta* **70**, 993–1019.

Touboul M., Puchtel I. S. and Walker R. J. (2012) ^{182}W evidence for long-term preservation of early mantle differentiation products. *Science* **335**, 1065–1069.

Touboul M., Kleine T., Bourdon B., Palme H. and Wieler R. (2007) Late formation and prolonged differentiation of the Moon inferred from W isotopes in lunar metals. *Nature* **450**, 1206–1209.

Trieloff M., Kunz J., Clague D. A., Harrison D. and Allegre C. J. (2000) The nature of pristine noble gases in mantle plumes. *Science* **288**, 1036–1038.

Wang Z. and Eiler J. M. (2008) Insights into the origin of low $\delta^{18}O$ basaltic magmas in Hawaii revealed from in situ measurements of oxygen isotope compositions of olivines. *Earth Planet. Sci. Lett.* **269**, 377–387.

Wang Z., Kitchen N. E. and Eiler J. M. (2003) Oxygen isotope geochemistry of the second HSDP core. *Geochem. Geophys. Geosyst.* **4**(8), 2002GC000406.

Wiechert U., Halliday A., Lee D.-C., Snyder G., Taylor L. and Rumble D. (2001) Oxygen isotopes and the Moon-forming giant impact. *Science* **294**, 345–348.

Workman R. K., Eiler J. M., Hart S. R. and Jackson M. G. (2008) Oxygen isotopes in Samoan lavas: confirmation of continent recycling. *Geology* **36**, 551–554.

Associate editor: Maud Boyet

Radiogenic isotope-$^{3}He/^{4}He$-$\delta^{18}O$ relationships for global geographical/geochemical affinities

In detail, $^{87}Sr/^{86}Sr$-$\varepsilon^{143}Nd$-$^{206}Pb/^{204}Pb$ compositions of high-$^{3}He/^{4}He$ samples are constant at a single location but vary slightly between locations (see Supplementary Information), consistent with the analysis of Jackson et al. (2007). Samples that approach endmember compositions, i.e. EM1 (Pitcairn, Rejuvenated Samoa, Hawaiian Koolau Component), EM2 (Malu Component Samoa), Kea trend, and HIMU do not have associated elevated $^{3}He/^{4}He$ values. In the case of EM1 (Samoa, Hawaiian Koolau Component) and EM2 (Malu Component Samoa), these endmembers also have $\delta^{18}O$ compositions that are elevated from the range observed for high-$^{3}He/^{4}He$ samples, although there is evidence that the EM1 component at Pitcairn has a $\delta^{18}O$ composition similar to the mean mantle (Eiler et al., 1995). The fact that high-$^{3}He/^{4}He$ locations have characteristic Sr-Nd-Pb-O isotopic compositions, and that Sr-Nd-Pb-O compositions are similar between high-$^{3}He/^{4}He$ locations, provides further indication that He and O remain coupled during melt production and melt migration processes. Coherent covariations of Sr-Nd-Pb-O-He are also observed within the Samoan and Loa trend datasets.

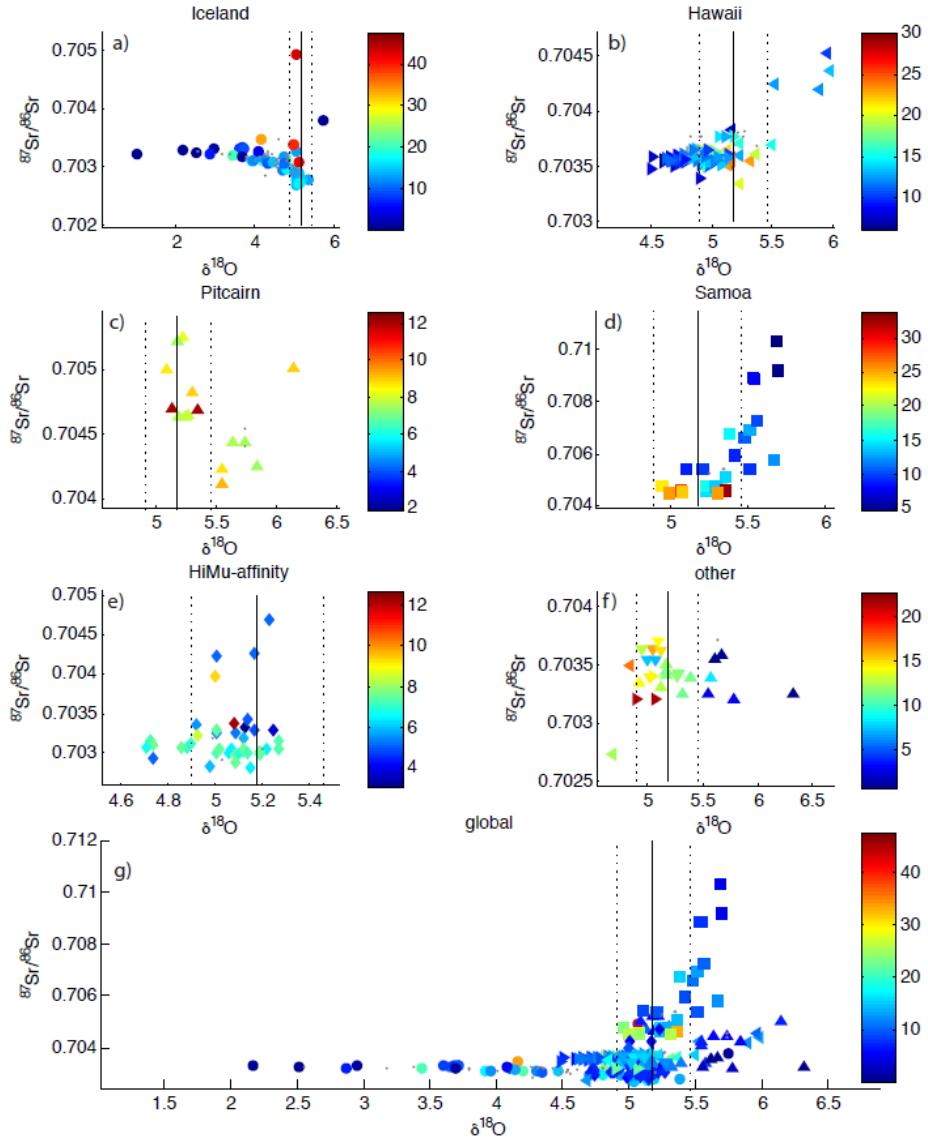

Supplementary Figure 1: $^{87}Sr/^{86}Sr$-$^{3}He/^{4}He$- $\delta^{18}O$ measurements plotted by a-f) geographic/geochemical affinities and g) as a global compilation (see reference list below). Data are colour-coded for $^{3}He/^{4}He$ values. Grey dots are used where no He data are available. Colour bars are rescaled so that the maximum $^{3}He/^{4}He$ value within that plot is the extreme red. High $^{3}He/^{4}He$ values generally cluster at a narrow range of $^{87}Sr/^{86}Sr$ and $\delta^{18}O$ values within individual geographic/geochemical affinities despite a wide range of $^{87}Sr/^{86}Sr$ values associated with lower $^{3}He/^{4}He$ samples. High $^{3}He/^{4}He$ samples from different geographic/geochemical affinities share similar $^{87}Sr/^{86}Sr$ values.

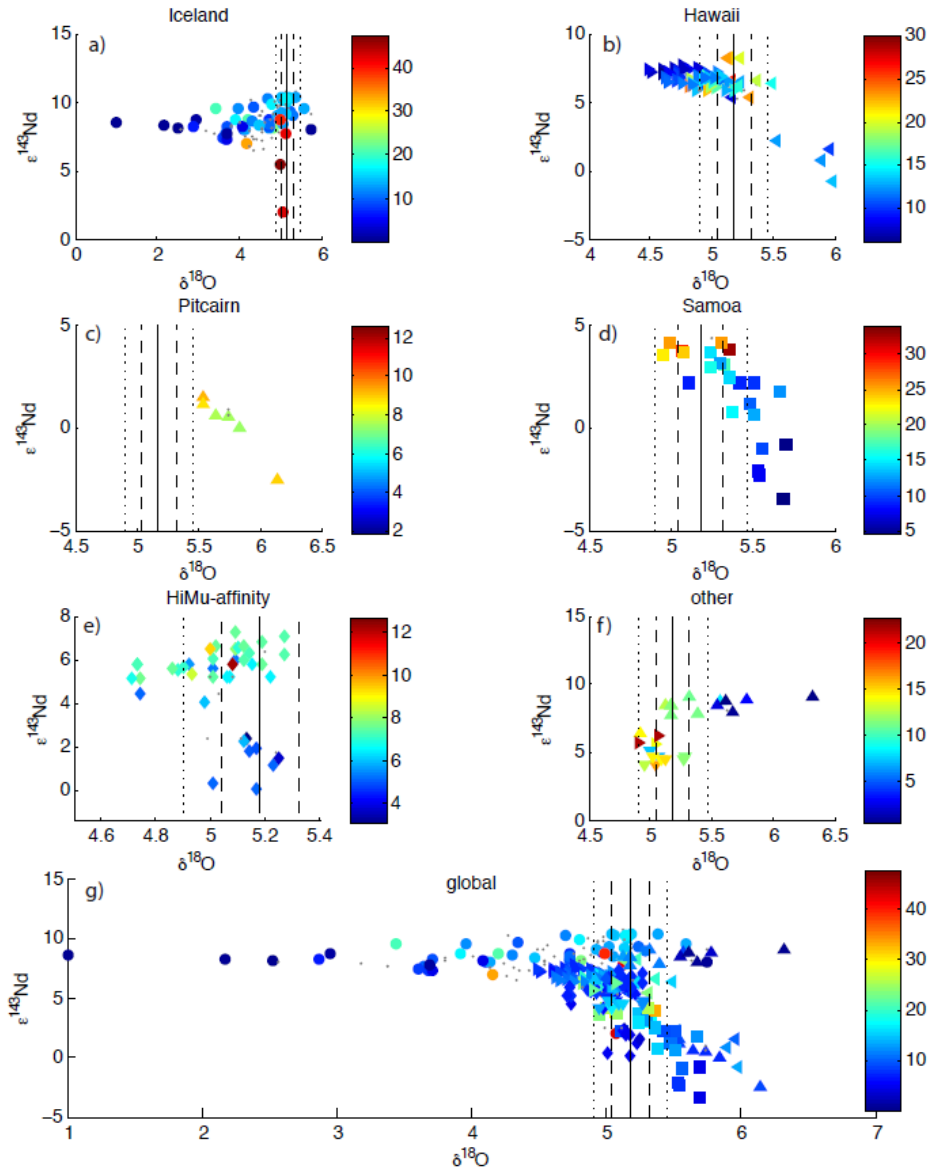

Supplementary Figure 2: $\varepsilon^{143}Nd$-$^{3}He/^{4}He$-$\delta^{18}O$ measurements plotted by a-f) geographic/geochemical affinities and g) as a global compilation (see reference list below). Data are color-coded for $^{3}He/^{4}He$ values. Grey dots are used where no He data are available. Colour bars are rescaled so that the maximum $^{3}He/^{4}He$ value within that plot is the extreme red. High $^{3}He/^{4}He$ values generally cluster at a narrow range of $\varepsilon^{143}Nd$ and $\delta^{18}O$ values within individual geographic/geochemical affinities despite a wide range of $\varepsilon^{143}Nd$ values associated with lower $^{3}He/^{4}He$ samples. High $^{3}He/^{4}He$ samples from different geographic/geochemical affinities share similar $\varepsilon^{143}Nd$ values.

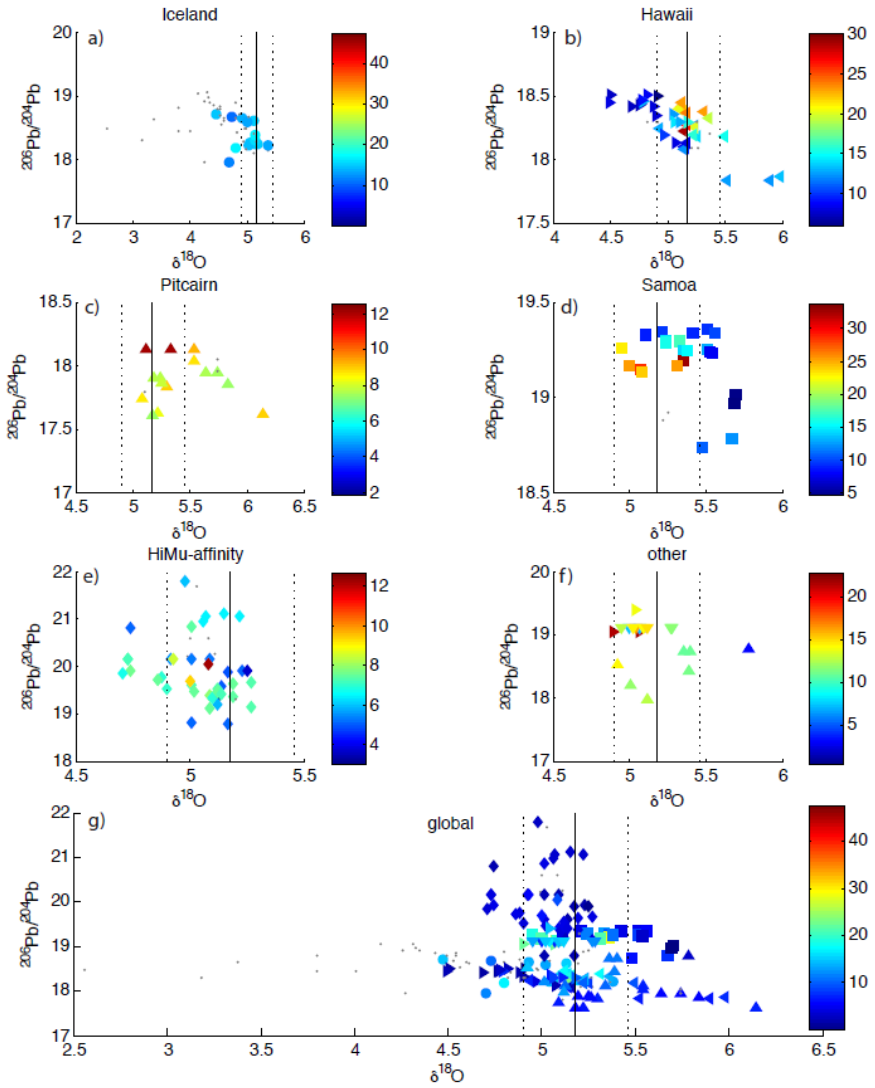

Supplementary Figure 3: $^{206}Pb/^{204}Pb$-$^{3}He/^{4}He$-$\delta^{18}O$ measurements plotted by a-f) geographic/geochemical affinities and g) as a global compilation (see reference list below). Data are colour-coded for $^{3}He/^{4}He$ values. Grey dots are used where no He data are available. Colour bars are rescaled so that the maximum $^{3}He/^{4}He$ value within that plot is the extreme red. High $^{3}He/^{4}He$ values generally cluster at a narrow range of $^{206}Pb/^{204}Pb$ and $\delta^{18}O$ values within individual geographic/geochemical affinities despite a wide range of $^{206}Pb/^{204}Pb$ values associated with lower $^{3}He/^{4}He$ samples. High $^{3}He/^{4}He$ samples from different geographic/geochemical affinities share similar $^{206}Pb/^{204}Pb$ values.

Compilation References:

Iceland:

Breddam, K., Kurz, M.D., Storey, M., 2000. Mapping out the conduit of the Iceland mantle plume with helium isotopes. Earth and Planetary Science Letters 176, 45-55.

Burnard, P., Harrison, D., 2005. Argon isotope constraints on modification of oxygen isotopes in Iceland Basalts by surficial processes. Chemical geology 216, 143-156.

Condomines, M., Grönvold, K., Hooker, P., Muehlenbachs, K., O'Nions, R., Oskarsson, N., Oxburgh, E., 1983. Helium, oxygen, strontium and neodymium isotopic relationships in Icelandic volcanics. Earth and Planetary Science Letters 66, 125-136.

Hilton, D.R., Thirlwall, M.F., Taylor, R.N., Murton, B.J., Nichols, A., 2000. Controls on magmatic degassing along the Reykjanes Ridge with implications for the helium paradox. Earth and Planetary Science Letters 183, 43-50.

Macpherson, C.G., Hilton, D.R., Day, J.M.D., Lowry, D., Grönvold, K., 2005. High-$^{3}He/^{4}He$, depleted mantle and low-[delta]18O, recycled oceanic lithosphere in the source of central Iceland magmatism. Earth and Planetary Science Letters 233, 411-427.

Skovgaard, A.C., Storey, M., Baker, J., Blusztajn, J., Hart, S.R., 2001. Osmium–oxygen isotopic evidence for a recycled and strongly depleted component in the Iceland mantle plume. Earth and Planetary Science Letters 194, 259-275.

Starkey, N.A., Fitton, J.G., Stuart, F.M., Larsen, L.M., 2012. Melt inclusions in olivines from early Iceland plume picrites support high $^{3}He/^{4}He$ in both enriched and depleted mantle. Chemical Geology 306, 54-62.

Starkey, N.A., Stuart, F.M., Ellam, R.M., Fitton, J.G., Basu, S., Larsen, L.M., 2009. Helium isotopes in early Iceland plume picrites: Constraints on the composition of high $^{3}He/^{4}He$ mantle. Earth and Planetary Science Letters 277, 91-100.

Stuart, F.M., Lass-Evans, S., Godfrey Fitton, J., Ellam, R.M., 2003. High $^{3}He/^{4}He$ ratios in picritic basalts from Baffin Island and the role of a mixed reservoir in mantle plumes. Nature 424, 57-59.

Thirlwall, M.F., Gee, M.A.M., Lowry, D., Mattey, D.P., Murton, B.J., Taylor, R.N., 2006. Low δ18O in the Icelandic mantle and its origins: Evidence from Reykjanes Ridge and Icelandic lavas. Geochimica et Cosmochimica Acta 70, 993-1019.

Thirlwall, M.F., Gee, M.A.M., Taylor, R.N., Murton, B.J., 2004. Mantle components in Iceland and adjacent ridges investigated using double-spike Pb isotope ratios. Geochimica et Cosmochimica Acta 68, 361-386.

Hawaii:

Blichert-Toft, J., Weis, D., Maerschalk, C., Agranier, A., Albarède, F., 2003. Hawaiian hot spot dynamics as inferred from the Hf and Pb isotope evolution of Mauna Kea volcano. Geochemistry, Geophysics, Geosystems 4.

Bryce, J.G., DePaolo, D.J., Lassiter, J.C., 2005. Geochemical structure of the Hawaiian plume: Sr, Nd, and Os isotopes in the 2.8 km HSDP-2 section of Mauna Kea volcano. Geochemistry, Geophysics, Geosystems 6.

Eiler, J.M., Farley, K.A., Valley, J.W., Hofmann, A.W., Stolper, E.M., 1996a. Oxygen isotope constraints on the sources of Hawaiian volcanism. Earth and Planetary Science Letters 144, 453-467.

Eiler, J.M., Valley, J.W., Stolper, E.M., 1996b. Oxygen isotope ratios in olivine from the Hawaii Scientific Drilling Project. Journal of Geophysical Research: Solid Earth (1978–2012) 101, 11807-11813.

Hauri, E.H., Lassiter, J.C., DePaolo, D.J., 1996. Osmium isotope systematics of drilled lavas from Mauna Loa, Hawaii. Journal of Geophysical Research: Solid Earth (1978–2012) 101, 11793-11806.

Kurz, M.D., Curtice, J., Lott, D.E., Solow, A., 2004. Rapid helium isotopic variability in Mauna Kea shield lavas from the Hawaiian Scientific Drilling Project. Geochemistry, Geophysics, Geosystems 5.

Kurz, M.D., Garcia, M.O., Frey, F.A., O'brien, P., 1987. Temporal helium isotopic variations within Hawaiian volcanoes: basalts from Mauna Loa and Haleakala. Geochimica et Cosmochimica Acta 51, 2905-2914.

Kurz, M.D., Jenkins, W.J., Hart, S.R., Clague, D., 1983. Helium isotopic variations in volcanic rocks from Loihi Seamount and the Island of Hawaii. Earth and Planetary Science Letters 66, 388-406.

Kurz, M.D., Kenna, T.C., Lassiter, J., DePaolo, D., 1996. Helium isotopic evolution of Mauna Kea Volcano: First results from the 1-km drill core. Journal of Geophysical Research: Solid Earth (1978–2012) 101, 11781-11791.

Roden, M., Trull, T., Hart, S., Frey, F., 1994. New He, Nd, Pb, and Sr isotopic constraints on the constitution of the Hawaiian plume: results from Koolau Volcano, Oahu, Hawaii, USA. Geochimica et Cosmochimica Acta 58, 1431-1440.

Wang, Z., Eiler, J.M., 2008. Insights into the origin of low δ18O basaltic magmas in Hawaii revealed from in situ measurements of oxygen isotope compositions of olivines. Earth and Planetary Science Letters 269, 377-387.

Wang, Z., Kitchen, N.E., Eiler, J.M., 2003. Oxygen isotope geochemistry of the second HSDP core. Geochemistry, Geophysics, Geosystems 4.

Pitcairn:

Eiler, J.M., Farley, K.A., Valley, J.W., Hauri, E., Craig, H., Hart, S.R., Stolper, E.M., 1997. Oxygen isotope variations in ocean island basalt phenocrysts. Geochimica et Cosmochimica Acta 61, 2281-2293.

Eiler, J.M., Farley, K.A., Valley, J.W., Stolper, E.M., Hauri, E.H., Craig, H., 1995. Oxygen isotope evidence against bulk recycled sediment in the mantle sources of Pitcairn Island lavas. Nature 377, 138-141.

Honda, M., Woodhead, J.D., 2005. A primordial solar-neon enriched component in the source of EM-I-type ocean island basalts from the Pitcairn Seamounts, Polynesia. Earth and Planetary Science Letters 236, 597-612.

Woodhead, J.D., Greenwood, P., Harmon, R.S., Stoffers, P., 1993. Oxygen isotope evidence for recycled crust in the source of EM-type ocean island basalts. Nature 362, 809-813.

Samoa:

Eiler, J.M., Farley, K.A., Valley, J.W., Hauri, E., Craig, H., Hart, S.R., Stolper, E.M., 1997. Oxygen isotope variations in ocean island basalt phenocrysts. Geochimica et Cosmochimica Acta 61, 2281-2293.

Jackson, M.G., Hart, S.R., Koppers, A.A., Staudigel, H., Konter, J., Blusztajn, J., Kurz, M., Russell, J.A., 2007a. The return of subducted continental crust in Samoan lavas. Nature 448, 684-687.

Jackson, M.G., Kurz, M.D., Hart, S.R., 2009. Helium and neon isotopes in phenocrysts from Samoan lavas: Evidence for heterogeneity in the terrestrial high $^{3}He/^{4}He$ mantle. Earth and Planetary Science Letters 287.

Jackson, M.G., Kurz, M.D., Hart, S.R., Workman, R.K., 2007b. New Samoan lavas from Ofu Island reveal a hemispherically heterogeneous high $^{3}He/^{4}He$ mantle. Earth and Planetary Science Letters 264, 360-374.

Workman, R.K., Eiler, J.M., Hart, S.R., Jackson, M.G., 2008. Oxygen isotopes in Samoan lavas: Confirmation of continent recycling. Geology 36, 551-554.

Workman, R.K., Hart, S.R., Jackson, M., Regelous, M., Farley, K., Blusztajn, J., Kurz, M., Staudigel, H., 2004. Recycled metasomatized lithosphere as the origin of the Enriched Mantle II (EM2) end-member: Evidence from the Samoan Volcanic Chain. Geochemistry, Geophysics, Geosystems 5.

HIMU-affinity:

Day, J., Peters, B.J., Janney, P.E., 2014. Oxygen isotope systematics of South African olivine melilitites and implications for HIMU mantle reservoirs. Lithos.

Day, J.M., Hilton, D.R., Pearson, D.G., Macpherson, C.G., Kjarsgaard, B.A., Janney, P.E., 2005. Absence of a high time-integrated $^{3}He/(U+ Th)$ source in the mantle beneath continents. Geology 33, 733-736.

Day, J.M.D., Hilton, D.R., 2011. Origin of $^{3}He/^{4}He$ ratios in HIMU-type basalts constrained from Canary Island lavas. Earth and Planetary Science Letters 305, 226-234.

Day, J.M.D., Pearson, D.G., Macpherson, C.G., Lowry, D., Carracedo, J.C., 2010. Evidence for distinct proportions of subducted oceanic crust and lithosphere in HIMU-type mantle beneath El Hierro and La Palma, Canary Islands. Geochimica et Cosmochimica Acta 74, 6565-6589.

Eiler, J.M., Farley, K.A., Valley, J.W., Hauri, E., Craig, H., Hart, S.R., Stolper, E.M., 1997. Oxygen isotope variations in ocean island basalt phenocrysts. Geochimica et Cosmochimica Acta 61, 2281-2293.

Janney, P., AP LE, R., Carlson, R., Viljoen, K., 2002. A chemical and multi-isotope study of the Western Cape olivine melilitite province, South Africa: implications for the sources of kimberlites and the origin of the HIMU signature in Africa. Journal of Petrology 43, 2339-2370.

Lassiter, J.C., Blichert-Toft, J., Hauri, E.H., Barsczus, H.G., 2003. Isotope and trace element variations in lavas from Raivavae and Rapa, Cook–Austral islands: constraints on the nature of HIMU- and EM-mantle and the origin of mid-plate volcanism in French Polynesia. Chemical Geology 202, 115-138.

Parai, R., Mukhopadhyay, S., Lassiter, J.C., 2009. New constraints on the HIMU mantle from neon and helium isotopic compositions of basalts from the Cook–Austral Islands. Earth and Planetary Science Letters 277, 253-261.

Other:

Eiler, J.M., Farley, K.A., Valley, J.W., Hauri, E., Craig, H., Hart, S.R., Stolper, E.M., 1997. Oxygen isotope variations in ocean island basalt phenocrysts. Geochimica et Cosmochimica Acta 61, 2281-2293.

Geist, D., Naumann, T., Larson, P., 1998. Evolution of Galápagos magmas: mantle and crustal fractionation without assimilation. Journal of Petrology 39, 953-971.

Hilton, D.R., Hammerschmidt, K., Loock, G., Friedrichsen, H., 1993. Helium and argon isotope systematics of the central Lau Basin and Valu Fa Ridge: Evidence of crust/mantle interactions in a back-arc basin. Geochimica et Cosmochimica Acta 57, 2819-2841.

Kurz, M.D., Geist, D., 1999. Dynamics of the Galapagos hotspot from helium isotope geochemistry. Geochimica Et Cosmochimica Acta 63, 4139-4156.

Macpherson, C.G., Hilton, D.R., Mattey, D.P., Sinton, J.M., 2000. Evidence for an ^{18}O-depleted mantle plume from contrasting $^{18}O/^{16}O$ ratios of back-arc lavas from the Manus Basin and Mariana Trough. Earth and Planetary Science Letters 176, 171-183.

Macpherson, C.G., Hilton, D.R., Sinton, J.M., Poreda, R.J., Craig, H., 1998. High $^{3}He/^{4}He$ ratios in the Manus backarc basin: Implications for mantle mixing and the origin of plumes in the western Pacific Ocean. Geology 26, 1007-1010.

Révillon, S., Chauvel, C., Arndt, N.T., Pik, R., Martineau, F., Fourcade, S., Marty, B., 2002. Heterogeneity of the Caribbean plateau mantle source: Sr, O and He isotopic compositions of olivine and clinopyroxene from Gorgona Island. Earth and Planetary Science Letters 205, 91-106.

Sinton, J.M., Ford, L.L., Chappell, B., McCulloch, M.T., 2003. Magma genesis and mantle heterogeneity in the Manus back-arc basin, Papua New Guinea. Journal of Petrology 44, 159-195.